The Leachability of Metals from Sedimentary Rocks

J.W. Lydon

Geological Survey of Canada, 601 Booth Street, Ottawa, ON, K1A 0E8
jlydon@nrcan.gc.ca

Abstract

Most models for SEDimentary EXhalative (SEDEX) and Mississippi Valley-type (MVT) ore systems envisage that metals were derived from the rocks of the sedimentary basins with which the deposits are spatially associated. To test whether sedimentary rocks could be the source for the ore metals and whether there are leaching windows during the course of burial, the leachability of metals and other elements has been measured on forty core samples of marine sedimentary rocks that represent burial depths ranging from 1 m to 20 km. The samples were taken along a transect across western Canada, and range in age from modern Pacific Ocean sediments to Mesoproterozoic siliciclastic rocks of the Belt-Purcell Basin. Four sequential leaches and an aqua regia leach of the samples were chemically analysed by ICP-MS and ICP-ES methods. Solid starting materials and leach residues were analysed for bulk chemistry by total dissolution and ICP-MS methods and for mineralogy by bulk XRD.

The contents of the metals that are commonly associated with SEDEX and MVT ore deposits (Zn, Pb, Cu, Ba, Mn) range over two orders of magnitude. A major cause for the variation of metal contents is the dilution of argillaceous and carbonaceous matter by quartz and carbonates. There is not an obvious correlation between metal content and depth of burial for these metals.

The first three sequential leaches by ammonium acetate, sodium pyrophosphate, and hydroxylamine, which purportedly extract only the labile metal content adsorbed on to clays, organic material and iron/manganese oxides, respectively, collectively leach on average 13% of the Zn, 33% of the Pb, 17% of the Cu, 10% of the Ba, 11% of the Fe and 22% of the Mn of the rocks. The fourth sequential leach by 1M HCl, dissolves most carbonates and monosulphides. The first three sequential leaches also solubilized on average about 50% of the Ca, 30% of the Mg, 20% of the Fe, and 5% of the K, which suggests that these leaches are not confined to eluting loosely bound cations but also dissolve or alter major rock forming minerals. The ratio between the proportion of a specific metal leached and the proportion of a specific major cation leached is reasonably constant from sample to sample for most leaches, which indicates that most metals in sedimentary rocks are contained within the structure of the rock-forming minerals. Furthermore, considering the low reactive capacity of natural fluids at low water:rock ratios, the results indicate that ore fluids containing >1 ppm base metal can only be produced by leaching during metamorphic mineralogical transformations driven by increasing temperature and pressure during burial.

Introduction

SEDimentary EXhalative (SEDEX) and Mississippi Valley-type (MVT) deposits (e.g. Leach et al., 2005) have been, and continue to be, the major source for the world's Zn and Pb supply (e.g. Goodfellow and Lydon, 2007). Compositions of fluid inclusions from ore and gangue minerals from SEDEX and MVT deposits (e.g. Roedder, 1984; Samson and Russell, 1987; Viets et al., 1996; Emsbo, 2009) indicate that ore-fluids for both types of ore deposits were evaporated sea water (Figure 1). In terms of major elements, the compositions of the fluid inclusions are very similar to the Na-Ca-Cl formational brines of oil-producing sedimentary basins, which also may contain up to tens or even hundreds ppm Pb and Zn (e.g. Hitchon, 1966; Rittenhouse et al., 1969; Hitchon et al., 1971; Carpenter et al., 1974; Sverjensky, 1984; Kharaka et al., 1987). Most genetic models for SEDEX and MVT ore deposits (e.g. Russell et al., 1981; Lydon, 1983) envisage that such metalliferous formational brines were the ore-forming fluid. The fundamental difference between the current genetic models for the two deposit types is the different flow paths of fluid expulsion from the basin (Figure 2). SEDEX deposits formed as the result of the upward cross-stratal flow of formational brines to the sea floor where the metals were deposited as stratiform sulphide bodies at or below the sediment-water interface (e.g. Lydon, 1983). In contrast, MVT deposits formed by lateral flow of formational brines from the basin to carbonate rocks on its adjacent shelf (e.g. Cathles and Smith, 1983) where the metals were deposited as sulphides within cavities in the carbonate rocks.
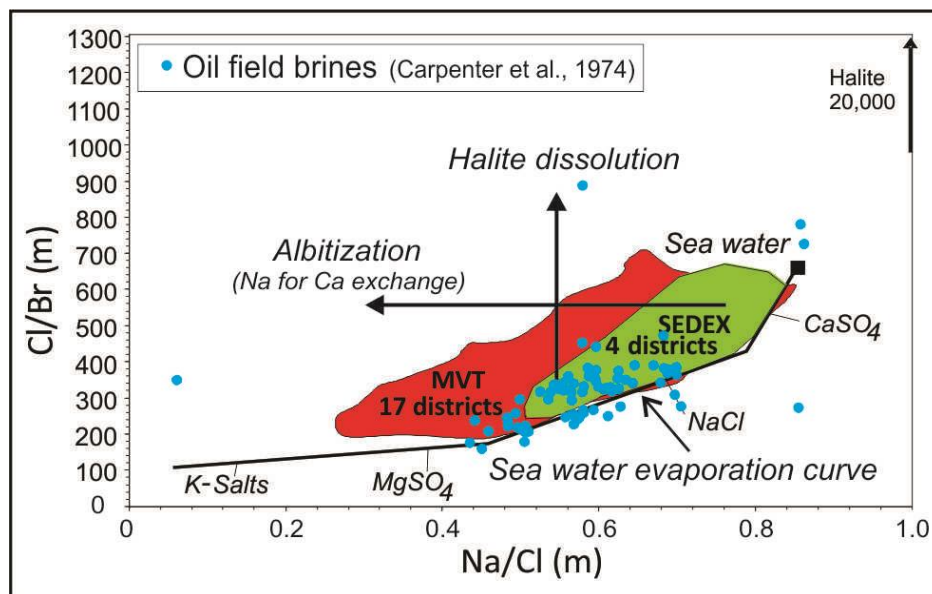

Figure 1. Fields for fluid inclusion compositions of ore minerals from SEDEX and MVT deposits (from Emsbo, 2009). Also plotted are data of Carpenter et al. (1974) for oil field brines in central Mississippi, US (blue dots). The similarity in compositions for all three populations suggests that the ore fluid for SEDEX/MVT ore systems are formational brines of sedimentary basins. Black square is modern sea water.
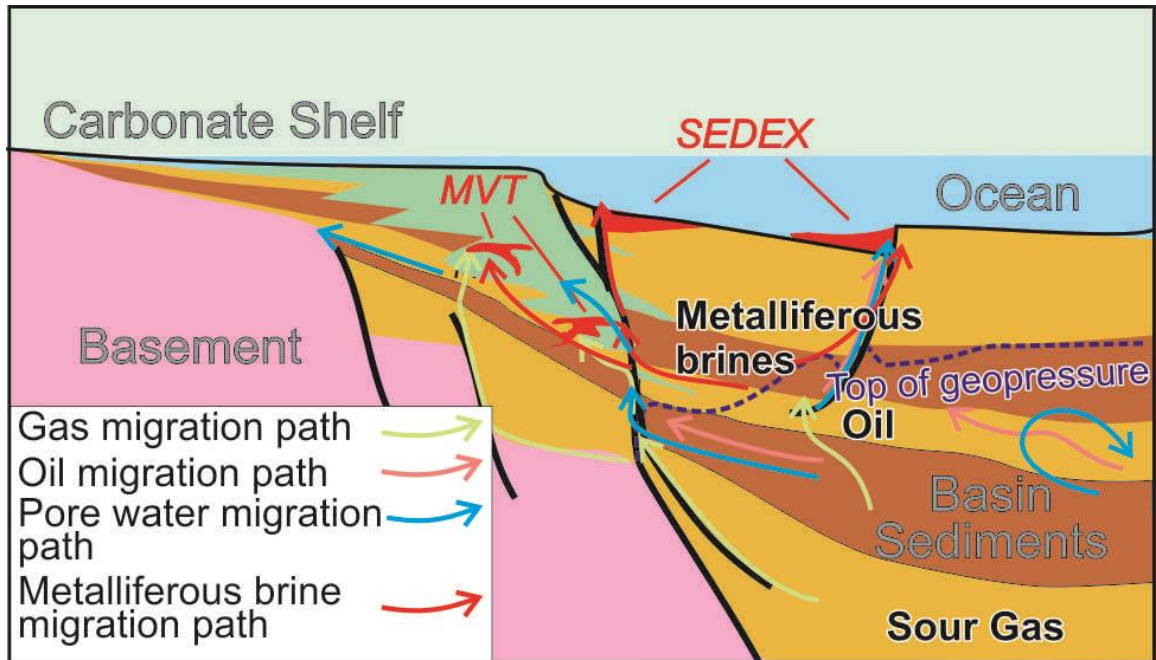
Figure 2. General model for SEDEX/MVT ore systems. Metalliferous brines are thought to exist in the deepest parts of sedimentary basins in the oil producing window but above the top of the geopressure boundary. At greater depths in the gas region, the second dehydration event of Burst (1969) is likely to dilute the brines, and the formation of sour gas likely precipitates metals as interstitial sulphides in the reservoir rocks. The main difference between genetic models for SEDEX and MVT deposits is that the brine expulsion is cross-stratal along synsedimentary faults to the contemporaneous seafloor for the former, but stratal and lateral into an adjacent carbonate shelf for the latter.

Irrespective of whether the mass flow of the formational fluids was caused by thermal convection (e.g. Russell, 1978; Yang et al., 2006), sediment compaction (e.g. Cathles and Smith, 1983), cross-stratal puncturing of geopressured reservoirs (e.g. Lydon, 1983), density-driven reflux of evaporitic brines (Emsbo, 2009), or topographically driven stratal flow (Garven and Freeze, 1985a and 1985b), the models assume that availability of metals is not an issue. Implicit in this assumption is that the brine will be able to elute or leach as much metal as is required to generate an ore-forming fluid before or during its migration to the site of ore deposition. This assumption seems to be supported by the empirical observation that most oil field brine samples containing >100,000 ppm Cl, also contain >1 ppm Zn (Figure 3) and >1ppm Pb (Hanor, 1996). The assumption also seems to be supported by experimental evidence. It has long been demonstrated that ore metals can be leached from sedimentary rock (e.g. Weiss and Amstutz, 1966; Ellis, 1968). More recently, Long and Angino (1982) used various chloride solutions to leach shales at temperatures of up to 90°C, their results indicating that up to 15% of the contained Zn and 100% of the contained Pb. could be leached. Zielenski et al. (1983) used a sequential series of weak selective leaches on Holocene-Pliocene red beds containing 31ppm to 110 ppm Zn and 12ppm to 37 ppm Pb. They found that about 20% of both metals were leached by

the sequential extractions and that most of this leached metal was that adsorbed on to iron oxide coatings of quartz grains. They concluded that red beds which are well flushed by suitable pore fluids (oxidizing or reducing) may be sources of significant quantities of heavy metals. Lentini and Shanks (1983) used various artificial chloride brines at 200°C to leach an arkose and also found that several to tens ppm metal could be liberated from the rock. Bischoff et al. (1981) reacted a graywacke with an artificial Na-Ca-K-Mg-Cl brine, similar in composition to a 130°C central Mississippi oil field brine, at temperatures of 200°C and 300°C. They concluded that metal solubilization by the brine followed the order of abundance in the graywacke: Zn > Ni > Cu > Pb > Sb > Cd, suggesting a common matrix and no selective leaching effect. In other words, as a given increment of rock was altered, all of its component metals were released. Importantly, these researchers, unlike the other works cited, also measured the concentrations of major element cations in the leachate as well as the trace metals, and also determined the mineralogy of solid reactants and products. Their results allowed the interpretation that most of the metal leached was from illite and plagioclase during their alteration to chlorite-smectite and albite, respectively. Like other laboratory leaching experiments, Bischoff et al. (1981) used a high liquid to solid ratio (water/rock ratio) of 10:1 mass ratio. This is the reverse of a natural system, where, especially in sedimentary rocks undergoing burial, even at a high porosity of 20%, the water/rock is about 1:10. It has been calculated by Lydon (1986), that at these low water/rock ratios, if the leaching of metals require the metasomatic hydrothermal alteration of the source rock, then the leachate would lose its reactive capacity before any significant amount of metals could be leached. It is therefore uncertain whether the laboratory experimental results for the quantities of metal leached are directly applicable to natural systems.
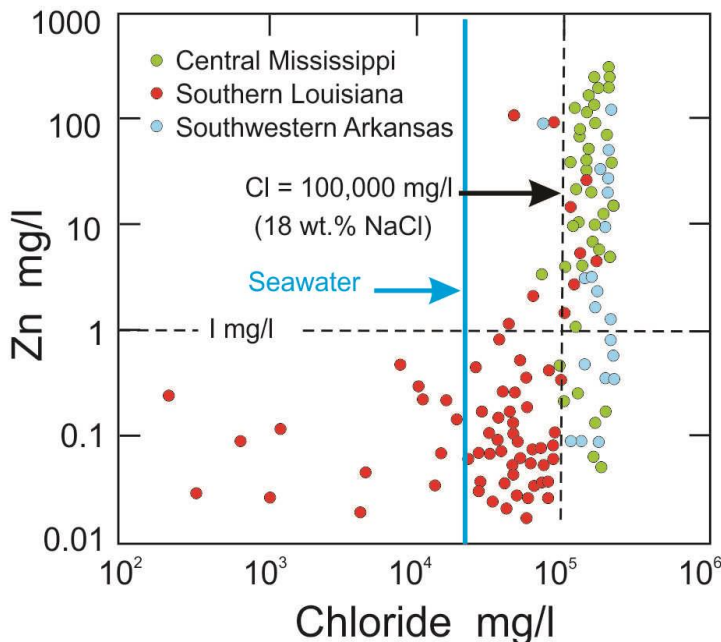

Figure 3. Relationship between concentrations of Zn and Cl in oil field brines of the USA. Modified after Hanor (1996).

A major knowledge gap in understanding SEDEX/MVT ore systems is how and when metalliferous brines of a sedimentary basin are generated. Can they be generated merely by brines being introduced as pore waters into a sedimentary basin and eluting loosely bound metals or are there specific metal leaching windows during basin evolution which allows metals to be leached during alteration of rock-forming minerals? Knowing how and when the metals are leached into a brine provides the knowledge needed to formulate the criteria by which a basin can be tested for its potential of having generated a SEDEX/MVT ore system. Fundamental to understanding the processes and timing that can leach metals is knowledge of the siting of metals in sedimentary rocks at successive stages of their burial history.

Argillaceous rocks usually form the bulk of the sedimentary basins (Garrels and Mackenzie, 1971) which are the sources of ore fluids for SEDEX and MVT deposits. The purpose of the study reported here was to determine the leachability and siting of base metals in argillaceous rocks of marine sedimentary basins in order to:
1. Determine whether argillaceous rocks are a viable source for ore metals in hydrothermal systems responsible for the formation of SEDEX and MVT deposits.
2. Determine whether argillaceous rocks have different degrees of susceptibility to metal leaching at different stages of burial metamorphism.
3. Use the results of the study to refine genetic models for SEDEX and MVT ore systems.

Methodology
Theoretical background
It has long been recognized (e.g. Turekian and Wedepohl, 1961) that metals may occur in rocks as:

i)   diadochic substitutions for major elements in rock forming minerals;
ii)   metallic mineral micro-inclusions in rock forming minerals;
iii) metallic minerals interstitial to rock forming minerals;
iv) adsorptions on to clays, iron and manganese oxides, organic matter.

Although the most direct determination of the form and siting of metals in rocks would be high precision micro-analysis of rock forming minerals and their intergranular regions, this method would be prohibitively time-consuming and expensive for a large number of samples of varied mineralogy. It was decided that a method of wet chemical sequential partial extractions would be more practicable and more closely simulate the natural leachability of metals. To facilitate interpretation of the leaching data, chemical and X-Ray diffraction (XRD) analysis of starting solid material and residues were also carried out, augmented by Scanning Electon Microscope (SEM) backscatter imagery, Energy Dispersive Spectrometry (EDS) and X-Ray mapping of grain mounts.

Interpretations of the results are based on the understanding that metals occurring within rock forming minerals (i and ii above) can only be leached to the extent of the reactive capacity of the solvent to alter/dissolve the host minerals and to the saturation limit of the metal in the leachate. Metals that are in metallic mineral interstitial to rock forming minerals or loosely bound to grain surfaces within the rock (iii and iv above) can be leached to the extent of saturation of the metal in the leachate.

Sample Collection

Forty core of marine argillaceous rocks were collected along a transect across western Canada (Figure 4), that range in age from modern ocean floor sediments to the Mesoproterozoic (Table 1) and represent burial depths that range from 1 m to 20 km. Modern ocean floor muds are from Middle Valley (Pacific Ocean) collected by piston coring in 1989. Samples collected along a transect across the Western Canada Sedimentary Basin, from eastern Saskatchewan to eastern British Columbia, are from oil well cores and range in age from Upper Cretaceous to Devonian. Other Paleozoic samples are from the White River Trough of eastern British Columbia, two of which are from outcrops. Mesoproterozoic samples are from the Purcell Basin, two of which are from outcrops.
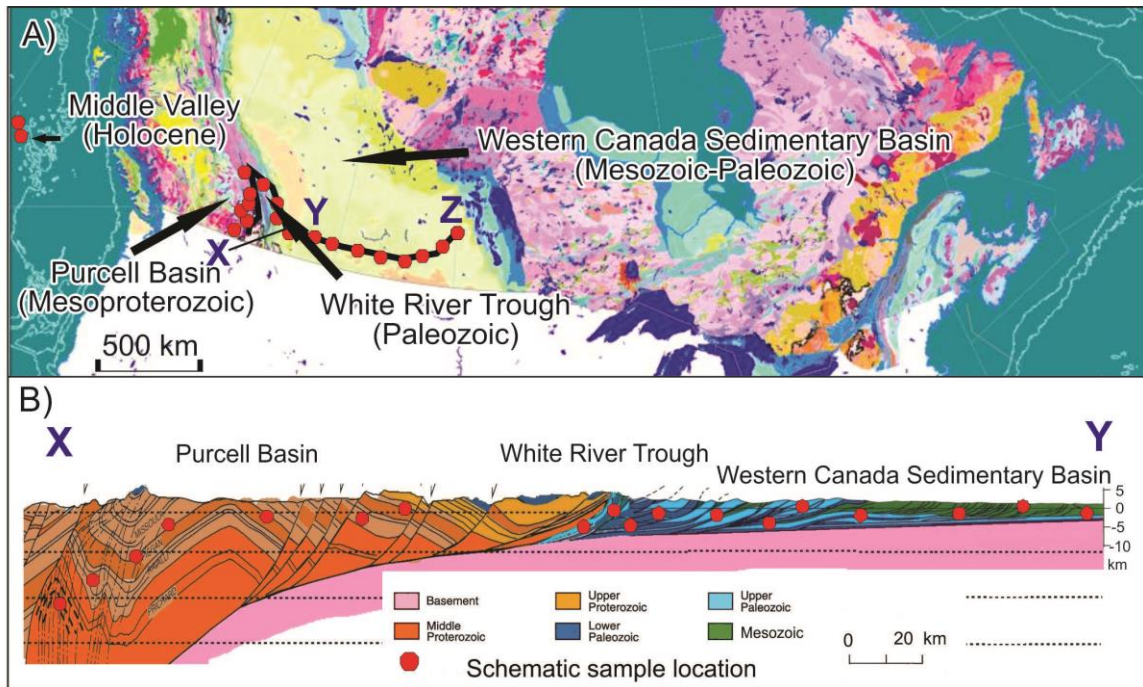

Figure 4. A) Geological map of the southern part of Canada showing schematic locations of samples used in this study. Accurate coordinates for the samples are given in Table 1. B) Geological cross section across western margin of the Western Canada Sedimentary Basin showing the schematic stratigraphic positions of samples used in this study.

Sample No	Depth (metres)	Formation	Period	Latitude (dd)	Longitude (dd)
LEA-89-TUL89D-28-0.5	0.5	Modern	Holocene	48.43330	-128.68080
LEA-89-TUL89D-28-5.3	5.3	Modern	Holocene	48.43330	-128.68080
LEA-12-Sask-8A	184.0	Lea Park	Cretaceous	52.10709	-102.44596
LEA-12-Sask-8B	223.0	Lea Park	Cretaceous	52.10709	-102.44596
LEA-12-ALB-1	201.5	Bearpaw Fm	Cretaceous	51.31125	-112.47107
LEA-12-ALB-3	576.0	Second W.S.	Cretaceous	50.35571	-110.55800
LEA-12-ALB-4	2,061.2	Second W.S.	Cretaceous	52.26396	-114.60415
LEA-12-ALB-8	1,783.8	Second W.S.	Cretaceous	52.91410	-116.10806
LEA-12-BC-1	1,066.1	Kaskapau	Cretaceous	54.93537	-120.09825
LEA-12-Sask-7A	2,072.0	Jolifu	Cretaceous	50.76796	-105.38921
LEA-12-Sask-2	667.3	Rierdon	Jurassic	50.26643	-101.91061
LEA-12-Sask-3	1,638.5	Rierdon	Jurassic	49.56910	-109.96514
LEA-12-ALB-7	2,185.3	Fernie Grp	Jurassic	53.53329	-115.09708
LEA-12-BC-2A	1,098.9	Fernie	Jurassic	56.41179	-120.06031
LEA-12-BC-3	2,320.8	Fernie	Jurassic	55.55308	-120.36790
LEA-12-FP3_578	578.0	Fernie	Jurassic	49.87623	-114.84406
LEA-12-Sask-5	0.0	Ashern	Devonian	52.69464	-104.98147
LEA-12-Sask-6A	1,037.3	Baakken	Devonian	49.71911	-101.56700
LEA-12-Sask-6B	1,038.7	Baakken	Devonian	49.71911	-101.56700
LEA-12-ALB-2	661.0	Ireton Fm	Devonian	52.81785	-110.52970
LEA-12-ALB-5	2,662.5	Ireton Fm	Devonian	55.03767	-117.45399
LEA-12-BC-6	1,959.0	Ireton	Devonian	58.07510	-121.89841
LEA-12-BC-5	1,863.0	Fort Simpson	Devonian	59.68137	-120.83037
LEA-12-BC-4	3,809.6	Fort Simpson	Devonian	56.94566	-122.07196
LEA-12-052	0.0	Eckshaw	Devonian	49.62598	-114.64814
LEA-12-CK-07-19-26	26.5	Harrogate	Devonian	49.96129	-115.46362
LEA-12-036	0.0	Jubilee	Cambrian	50.13163	-115.49644
LEA-12-FN10-01_20.1	20.2	Chancellor	Cambrian	50.51172	-115.57444
LEA-12-FN-10-01-282	282.6	Chancellor	Cambrian	50.51172	-115.57444
LEA-12-BD_002-36.8	36.8	Dutch Creek	Mesoprot.	50.36081	-116.39161
LEA-12-JI-97-04	129.5	Dutch Creek	Mesoprot.	49.59417	-116.66056
LEA-12-354-8	8.0	Creston	Mesoprot.	49.74133	-115.96385
LEA-12-354-879	879.0	Creston	Mesoprot.	49.74133	-115.96385
LEA-12-Z-03-07	676.0	Creston	Mesoprot.	49.43149	-116.15823
LEA-12-SG- 07-05-133.2	133.2	U. Aldridge	Mesoprot.	49.27432	-115.80716
LEA-08-239	239.0	M. Aldridge	Mesoprot.	49.72804	-115.58697
LEA--10-SD2-2461	2,461.0	L. Aldridge	Mesoprot.	49.75374	-116.03258
LEA-12-6406-192	192.0	M. Aldridge	Mesoprot.	49.71357	-115.89618
LEA-12-6423-1065	1,065.0	L. Aldridge	Mesoprot.	49.69374	-115.94598
LEA-12-ED2012-29	0.0	L. Aldridge	Mesoprot.	49.64189	-116.10593

Table 1. Stratigraphic position, geographic location and brief geological description of samples used in this study.

Sample No	Description
LEA-89-TUL89D-28-0.5	Thin bedded argillaceous to sandy marine turbidite
LEA-89-TUL89D-28-5.3	Thin bedded argillaceous to sandy marine turbidite
LEA-12-Sask-8A	Greenish grey mudstone
LEA-12-Sask-8B	Grey to black mudstone
LEA-12-ALB-1	Massive but fissile medium grey argillite
LEA-12-ALB-3	Laminated carbonaceous shale with layers of light grey ash(?)
LEA-12-ALB-4	Laminated black shale with thin beds and lenses of siltstone.
LEA-12-ALB-8	Carbonaceous shale
LEA-12-BC-1	Carbonaceous siltite with layers of current-bedded arenite.
LEA-12-Sask-7A	Black shale and intercalated siltite
LEA-12-Sask-2	Very soft greenish grey argillite.
LEA-12-Sask-3	Medium grey, weakly calcareous argillite with shell fragments.
LEA-12-ALB-7	Slightly micaceous black shale with silty laminae
LEA-12-BC-2A	Carbonaceous shale.
LEA-12-BC-3	Carbonaceous argillite with layers of dolomitic siltstone.
LEA-12-FP3_578	Glauconitic shale with large belemnites
LEA-12-Sask-5	Massive brownish grey marl with carbonaceous layers.
LEA-12-Sask-6A	Black shale at top of core.
LEA-12-Sask-6B	Laminated green and white argillite. Not calcareous.
LEA-12-ALB-2	Greenish grey dolomite marl with oil in vugs
LEA-12-ALB-5	Massive fissile shale with scattered pyrite nodules
LEA-12-BC-6	Weakly calcareous carbonaceous argillaceous siltite.
LEA-12-BC-5	Carbonaceous shale.
LEA-12-BC-4	Slightly calcareous carbonaceous and argillaceous siltite.
LEA-12-052	Black Shale.
LEA-12-CK-07-19-26	Light buff to khaki coloured, fine grained marl.
LEA-12-036	Shale layer from a nodular carbonaceous carbonate
LEA-12-FN10-01_20.1	Black Shale
LEA-12-FN-10-01-282	Black Shale
LEA-12-BD_002-36.8	Micaceous siltite
LEA-12-JI-97-04	Black Argillite
LEA-12-354-8	Weakly Carbonaceous argillite
LEA-12-354-879	Grey argillite
LEA-12-Z-03-07	Thin bedded light grey argillite
LEA-12-SG- 07-05-133.2	Thin bedded argillite
LEA-08-239	Laminated siltite
LEA--10-SD2-2461	CWL - Carrbonaceous Wacke Laminite
LEA-12-6406-192	Argillaceous biotitic turbidite
LEA-12-6423-1065	Thin bedded biotitic chloritic turbidite.
LEA-12-ED2012-29	Muscovite-silliminite schist.

Table 1 (continued).

Sample Processing

A sample of about 300 grams was cut with a water-cooled diamond saw to produce a slab for a polished thick section and the remainder crushed in a SEPOR mini steel jaw crusher to <3 mm fragment size. Approximately 20 grams of the crushed sample was pulverized to a <200 micron in a tungsten carbide shatter-box for two minutes and separated into subsamples of about 15 grams for whole rock chemical analysis and 5 grams for XRD analysis. The remaining crushed sample was pulverized in a SEPOR mini pulverizer disc mill with tungsten carbide plates and dry sieved until 70 grams of a 60-100 mesh sized fraction was obtained for sequential and partial wet chemical leaching analysis. The 60-100 mesh fraction was quickly stirred into distilled water and decanted after 10 seconds of settling, to remove the >100 mesh rock dust that may have collected on the 60 mesh fragments. This washing protocol was exercised to mitigate against the faster reaction rates of the very small grain size of the dust being a dominant factor in controlling the amount of different elements leached from the crushed rock by different reagents. This process of "cleaning" could not be applied to the Middle Valley and some Mesozoic samples, because they disaggregated in water.

Chemical analyses were carried out by Acme Laboratories of Vancouver. The 60-100 micron size fraction was analysed using the sequential extraction methods described below, followed by Inductively Coupled Plasma Emission Spectrometry (ICP-ES) or Inductively Coupled Plasma Emission Spectrometry (ICP-MS) detection. The solid starting material and the residue from both the sequential and aqua regia leach were analysed by a four acid "near total" extraction followed by ICP-ES or ICP-MS detection. The unsieved >200 mesh powder was also analysed by the four acid "near total" dissolution method to determine whether the sieving had caused significant preferential mineral loss or concentration.

Sections intended for petrography and SEM investigations were prepared by Vanpetro of Vancouver. However, because of the generally unconsolidated nature of argillaceous samples in the study suite and the limited benefits of transmitted light petrography for such fine grained rocks, it was elected to make thick polished section material that could be used for SEM work. Determination of the mineralogy of samples and residues by XRD analysis was carried out in the Geological Survey of Canada's X-Ray laboratories at 601 Booth Street in Ottawa. SEM X-Ray mapping and EDS semi-quantitative analysis were carried out by the Geological Survey of Canada's SEM laboratory at 601 Booth Street in Ottawa.

Chemical analyses

Subsamples of the whole rock (original material), the 60-100 mesh fraction, the residue from the sequential leach process on the 60-100 mesh fraction and the residue from an aqua regia leach of the 60-100 mesh fraction were analysed for total abundances of Si, Al, Fe, Mg, Ca, Na, K, Ti, P, Cr, LOI, Ba, Y, and Zr by

Acme Method 4A which involves ICP-ES following a lithium metaborate/tetraborate fusion and dilute nitric digestion of a 0.2 gram sample. Total carbon and total sulphur were determined by infrared spectroscopy after ignition in a LECO furnace at 1000°C. Carbonate carbon was determined by direct CO_2 evolution by digestion with HCl and LECO analysis. Organic carbon was calculated by the difference between total and carbonate carbon and thus includes graphite as well as kerogen and bitumen. Loss on ignition (LOI) was determined by weight difference between a sample dried at 105°C and after ignition at 1000°C. Mn, S, Ag, As, Au, Be, Bi, Cd, Co, Cr, Cs, Cu, Ga, Hf, In, Li, Mo, Nb, Ni, Pb, Rb, Re, Sb, Sc, Se, Sn, Sr, Ta, Te, Th, Tl, U, V, W, Zn, and the REE (Ce, La, Pr, Nd, Sm, Eu, Gd, Tb, Dy, Ho, Er, Tm, Yb, Lu) were analysed by ICP-mass spectrometry after total or near total dissolution by a four acid (HF-$HClO_4$-HNO_3-HCl) digestion. Statistics for selected elements for both the unsieved and sieved starting materials are given in Table 2. Note that the abundances of elements are reported as parts per million of the element, including the major elements, which conventionally are reported as parts per cent of the oxide.

The leachates of 30 grams subsample of the 60-100 mesh fraction were analysed by ICP-MS following each stage of the following sequential leaches, which are reputed to be selective for the indicated cation sites (e.g. Chao, 1984):

- 1.0 M ammonium acetate leach for exchangeable cations adsorbed by clay and elements co-precipitated with carbonates,
- 0.1 M sodium pyrophosphate leach for elements adsorbed by organic matter (humic and fulvic compounds),
- 0.25 M hydroxylamine leach for elements adsorbed by amorphous Fe hydroxide and Mn hydroxide,
- 1.0 M warm hydrochloric acid for dissolution of carbonates and monosulphides.

A 15 grams subsample of the 60-100 mesh fraction was analysed by an aqua regia partial digestion followed by an ICP-MS analysis.

Results for all chemical analyses are reported in a separate Geological Survey of Canada Open File (Lydon et al., in preparation) and partially graphically represented here in Figures 5, 6 and 7.

XRD analysis
The mineralogy of a whole rock powder and clay-sized separates was determined by XRD Bulk samples were further micronized using a McCrone mill in isopropyl alcohol until a grain size of around 5-10 μm was achieved. Samples were left to dry overnight and then back-pressed into an aluminium holder to produce a specimen with random orientation. For clay-sized separates, 40 mg of the sample were suspended in distilled water and pipetted onto glass slides and air-dried to produce oriented mounts. X-ray patterns of the pressed powders and

	Si	Al	Fe	Mg	Ca	Na	K
MDL	*50*	*50*	*300*	*60*	*70*	*75*	*80*
Whole Rock							
MAX	353,334	121,093	73,090	122,356	214,479	25,223	47,401
MIN	10,003	2,117	3,008	1,749	214	74	581
AVERAGE	259,560	73,358	33,249	19,709	39,138	7,252	26,199
60-100 Mesh fraction							
MAX	353,755	121,516	57,423	118,014	216,980	27,523	46,820
MIN	15,192	4,552	3,987	1,869	429	148	1,411
AVERAGE	258,674	72,318	32,618	19,662	40,603	7,124	25,830

	Ti	P	S	Carbonate as C	C-org as C	Calc H$_2$O
MDL	*60*	*60*	*200*	*55*	*55*	
Whole Rock						
MAX	6,892	6,016	36,600	111,942	187,362	117,435
MIN	120	61	400	49	227	19,910
AVERAGE	3,732	1,086	7,323	14,240	16,388	50,283
60-100 Mesh fraction						
MAX	7,072	12,457	36,300	120,681	166,601	125,343
MIN	300	122	200	55	645	1,000
AVERAGE	3,722	1,331	7,500	15,983	14,100	49,037

	Ba	Cu	Mn	Ni	Pb	Zn
MDL	*5*	*0.02*	*2*	*0.2*	*0.02*	*0.2*
Whole Rock						
MAX	3,039	99	2,144	218	121	1,398
MIN	80	1	39	4	4	5
AVERAGE	673	29	398	40	23	128
60-100 Mesh fraction						
MAX	3,380	204	3,280	231	101	1,955
MIN	77	3	33	5	4	7
AVERAGE	652	35	440	41	23	147

Table 2. Statistics for major elements and the trace metals important to SEDEX/MVT ore systems for the whole rock and the 60-100 mesh fraction of the 40 samples used in this study. Note that all values are in ppm. MDL - minimum detection limit.

air-dried samples were recorded on a Bruker D8 Advance Powder Diffractometer equipped with a Lynx-Eye Detector, Co Kα radiation set at 40 kV and 40 mA. The oriented samples were also X-rayed following saturation with ethylene glycol and heat treatment (550ºC).
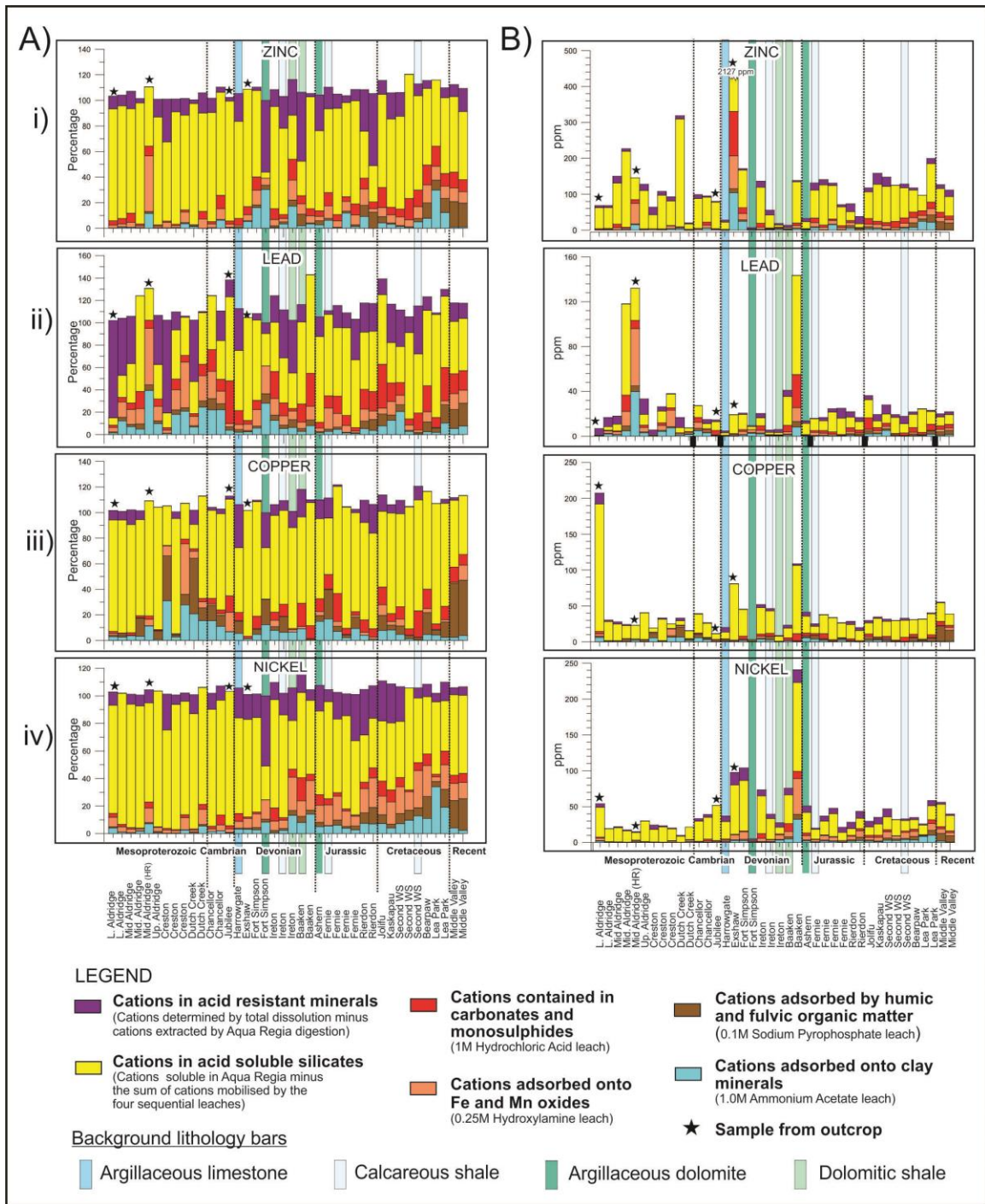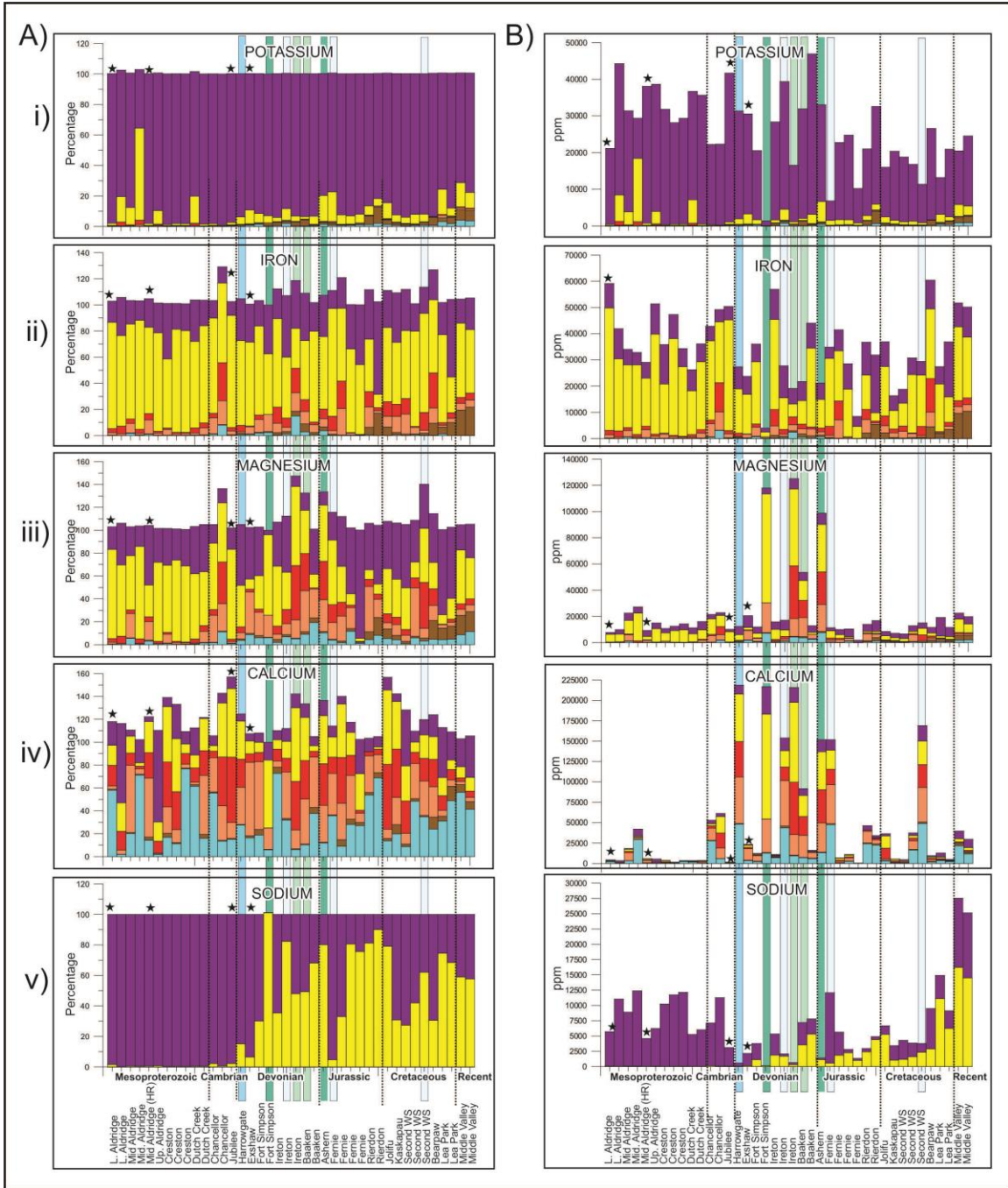
Figure 5. A) Relative proportions of selected metals in leachates and residues of argillaceous sedimentary rocks from Western Canada. The purported siting indicated by each leachate and residue is indicated in the legend. B) Contents of selected ore metals for the same argillaceous sedimentary rocks from Western Canada shown in A). Note that all contents are in ppm and that the samples are plotted from right to left in the same order as listed in Table 1. See text for discussion of results.

Figure 6. A) Relative proportions of selected major elements in leachates and residues of argillaceous sedimentary rocks from Western Canada. B) Contents of selected major elements for the same rocks shown in A). Note that all contents are in ppm. Legend is the same as in Figure 5. Sodium was analysed only in residues because of the use of sodium pyrophosphate in the sequential leach process. Silicon and aluminium were not analysed in leachates because of the low saturation levels of both these elements in the leachates. Note that all contents are in ppm and that the samples are plotted from right to left in the same order as listed in Table 1. See text for discussion of results.
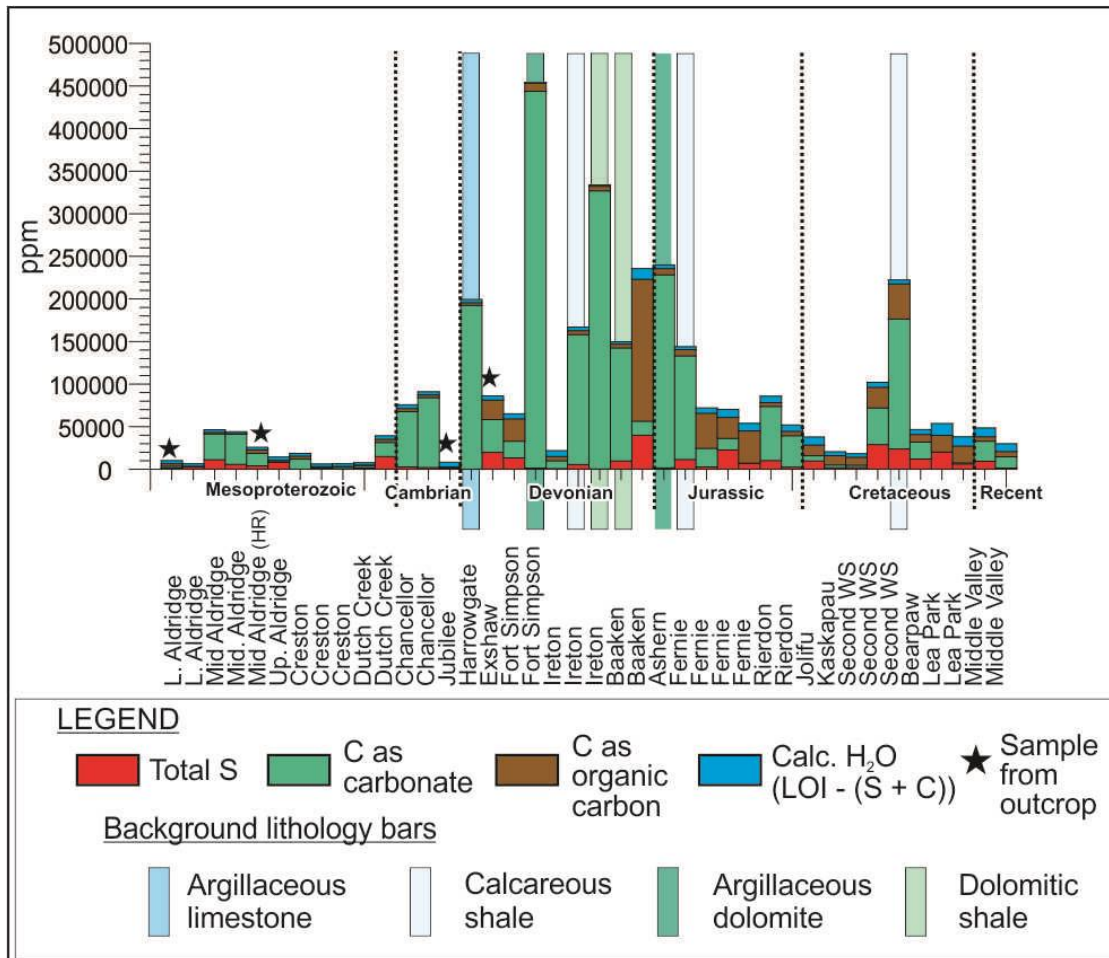
Figure 7. Contents of sulphur, carbonate carbon, organic carbon and calculated water in the 60-100 mesh fraction of argillaceous sedimentary rocks from western Canada. See text for discussion of results.

Initial identification of minerals was aided using EVA (Bruker AXS Inc.) software with comparison to reference mineral patterns using Powder Diffraction Files (PDF) of the International Centre for Diffraction Data (ICDD) and other available databases. Quantitative analysis is carried out using TOPAS (Bruker AXS Inc.), a PC-based program that performs Rietveld refinement (RR) of XRD spectra. This is based on a whole pattern fitting algorithm that relies on having particular mineralogical structure files (.cif) such that the reference minerals are as close a match to the unknown as possible.

SEM analysis

It was the intent to substantiate conclusions from the leaching experiment by examining polished grain mounts of the starting 60-100 mesh rock powders and leach residues by EDS and X-Ray mapping to identify the minerals that were leached and formed by the leaching reactions. However, it was found that the magnification required to identify corrosion and alteration of rock grains could not be achieved at the Geological Survey of Canada SEM laboratory, because of

vibration effects on the 7th floor of a building. SEM investigations to date have been limited to back scatter imaging and EDS semi-quantitative analysis at a resolution scale of about 1 micron.

Results/Data Analysis
Metal and major element contents and proportions

The contents of metals that are commonly associated with SEDEX and MVT ore deposits (Zn, Pb, Cu, Ba, Mn) range over two orders of magnitude in the argillaceous rocks analysed in this study (Table 2; Figure 5). The statistics indicate that on average dry sieving of the samples did not result in any consistent significant preferential loss or concentration for most elements, with element contents of the 60-100 mesh fraction being between 98% and 102% of the values determined for the whole rock. The major exceptions are for P and Cu whose average values are 120% higher in the 60-100 mesh fraction. Maximum values for most elements in the 60-100 mesh fraction are also between 98% and 102% of the values determined for the whole rock. The main exceptions are depletions of Fe and Pb (78% and 84%, respectively) and enrichments of P, Cu, Mn and Zn (207%, 205%, 150% and 140%, respectively), compared to contents of the unsieved whole rock. The reasons for these apparent depletions and enrichments in the 60-100 mesh fraction for the affected samples have not been determined.

The relative proportions of metals extracted by the four sequential leaches (ammonium acetate, sodium pyrophosphate, hydroxylamine, and hydrochloric acid successively) are calculated with respect to the total metal content of the sample (as determined by the total dissolution analysis of the 60-100 mesh fraction). The amount of metal in acid soluble minerals is calculated as the metal content extracted by the aqua regia leach minus the metal content extracted by the four sequential leaches, and its relative proportion calculated with respect to the total metal content of the sample. The amounts of metals in acid insoluble minerals is calculated by subtracting the metals extracted by the aqua regia leach from the total metal content, and its relative proportion calculated with respect to the total metal content of the sample. The relative proportions of metals in the different sites commonly sum to >100% for several reasons. Concentrations of metals below detection limits were assigned the value of the detections limit, and therefore in these cases the summation of the different extractions exceeds the measured total metal content. There may also be discrepancies in the calibration of the different instruments used for the total dissolution (ICP-MS) and partial leaches (ICP-ES) with the latter giving higher results for some elements. For some samples, there may also be the nugget effect for some metals in some samples where the metals occur as intergranular grains of sulphides. These nuggets are more likely to occur in the 30 grams of samples used for the sequential leaches than the 1 gram sample used for complete dissolution.

Generally, the major cause for variation of metal contents is dilution of argillaceous and carbonaceous matter by carbonates, and to some extent quartz.

That samples with the highest carbonate contents generally have the lowest metal contents can be seen by comparing metal contents shown in Figure 5, with Ca and Mg contents on Figure 6, and the carbonate carbon content shown on Figure 7. This comparison is aided by the background bars colour coded for rocks with elevated carbonate contents, i.e. argillaceous limestone, calcareous shales, argillaceous dolomite and dolomitic shale. High contents of single metals are most commonly due to the presence of an interstitial diagenetic sulphide, e.g. Cu in the stratigraphically lowest Mesoproterozoic Lower Aldridge sample (LEA-12-ED2012-29), Pb, and to some extent Zn, in the two Mesoproterozoic Middle Aldridge samples (LEA-08-239 which is near the Kootenay King SEDEX deposit, and LEA-12-6406-192, which is just 5 km east of the Sullivan deposit). Other high metal spikes may be attributable to unusually high contents of metal-trapping components such as the high Pb, Cu and Ni associated with the high organic carbon content of the stratigraphically highest sample of the Devonian Baaken Formation (LEA-12-Sask-6A). Others, specifically the very high Zn content of the Devonian Exshaw Formation, represent a regional enrichment of unknown geological significance (P. Ransom, personal communication, 2012).

For the metals plotted in Figure 5, there is not an obvious correlation between metal content and depth of burial, except in the case of Ni, which generally decreases with depth (Figure 5iv). This Ni trend is broadly similar to the organic carbon trend (Figure 7), suggesting that Ni (along with V) migrates with oil. For major elements (Figure 6) there is a general increase in K, Fe and Mg contents with depth of burial, perhaps reflecting the normal diagenetic progression of smectite to illite transformation, the chloritization/illitization of feldspar, and the upwards migration of carbonate and silica due to pressure solution, dewatering and interstitial cement evolution (e.g. Milliken, 2004). There is a general decrease in organic carbon, water and sulphur contents with depth (Figure 7) reflecting devolatilization with increasing temperature with increasing burial depth. However, burial related compositional changes are difficult to distinguish from provenance-related and depositional-environment factors for this data set, which spans 1500 my in age and >1000 km in current distance. The amount of carbonate in the samples, and consequently Ca and/or Mg, appears to largely reflect the depositional environment. Half the samples of Paleozoic age are elevated in carbonate content (Figure 7) reflecting their deposition in or near a carbonate shelf environment.

The first three sequential leaches, which purportedly do not involve the destruction of host minerals but extract only the labile metal content, collectively leach on average 20 ppm Zn, 8 ppm Pb, 6 ppm Cu, 68 ppm Ba, 3480 ppm Fe and 180 ppm Mn (Table 3 and Figure 5B). These amounts represent 13% of the Zn, 33% of the Pb, 17% of the Cu, 10% of the Ba, 11% of the Fe, and 22% of the Mn originally present in the rocks, which is similar to the proportions reported in the literature for both low temperature partial leaching of sedimentary rocks by weak selective leaches (Zielenski et al., 1983) and chloride brines (Long and Angino, 1982) and high temperature (> 200°C) brines (Bischoff et al., 1981;

Lentini and Shanks, 1983). The first three sequential leaches on average also solubilizes about 50% of the Ca, 30% of the Mg, 20% of the Fe, and 5% of the K (Figure 6). This suggests that these leaches, which supposedly leach only ions adsorbed on to minerals, in fact also significantly dissolves or alters the rock forming minerals. This means that at least a proportion of the metals extracted by the sequential leaches were likely contained in the structure of the rock forming minerals and not exclusively adsorbed on to the surfaces of clays, organic matter, and iron or manganese oxides. Thus this observation, and inferences that can be made from it, has very important consequences for both the interpretation of laboratory leaching experiments by partial extractions, but also on the assumptions of the selectivity of the leaches used in the work described here.

Siting of metals in marine argillaceous sediments
With the caveat of the inference, noted above, that the sequential selective leaches employed in this study may not be as specifically selective as they are purported to be, the data illustrated in the left hand columns of Figures 5 and 6 gives some insights into the siting of metals in marine argillaceous sediments. It is evident that in many cases, the relative proportions of elements frequently sum to >100%. The reasons for this have not been fully investigated, but there are several possibilities. A major reason could be that apportioning the elements to different sites relies on three different analytical procedures (sequential leach, aqua regia leach, and four acid "near total" dissolution), each with their own instrumentation and calibrations. Noting that the proportioning is relative to the four acid "near total" dissolution, an over estimation of the proportion of an element occurs if analysis of partial extraction leachates over-estimate the actual concentration. The discrepancies are most pronounced where the concentration of elements are close to the minimum detection limits of the method. The most pronounced discrepancies are for Pb among the metals and Ca among the major elements. Sodium was analysed only in residues, because of the use of sodium pyrophosphate in the sequential leach process. Silicon and aluminium were not analysed in leachates because of the low saturation levels of these elements in aqueous solutions.

Ammonium acetate leach – elements adsorbed by clay minerals
Considering that the samples were chosen for their argillaceous content, it was somewhat surprising that this leach generally extracted the smallest proportion of the sequential leaches. The leachable proportion is sporadic for Zn and Pb, but generally increases with increasing maximum burial depth for Cu until Aldridge Formation and generally decreases with maximum burial depth for Ni (Figure 5A). This leach generally does not extract more than 2% of major elements except for Ca (~20% and more) and Mg (up to 5%) (Figure 5A). These results suggest that the ammonium acetate leach attacks carbonates, particularly calcium carbonate.

Sodium pyrophosphate leach – elements adsorbed by organic matter

Although there are no strong correlations between any metal or major element and organic carbon, the proportion of metals (Figure 5A) and major elements (Figure 6A) extracted by this leach tends to decrease with increasing burial depth, mimicking the trend for whole rock organic carbon content (Figure 7). Of the major elements, Fe and Mg, and to a lesser extent K, are the most leachable, but only in rocks of Devonian age or younger. This may suggest that this leach also attacks smectite clays, chlorite and probably also calcite and dolomite.

Hydroxylamine leach – elements adsorbed by iron and manganese oxides

This leach fairly consistently extracts 5-10% of Zn, Pb and Cu, with the proportions tending to increase with the age of the rock. It also consistently extracts 10-20% of the Fe, 10-40% of the Mg, and 10-60% of the Ca but does not extract any significant amounts of K. Rocks with the lowest proportion of the major elements extracted by this leach are the youngest ones. The reason for this is unclear, but it may be that this leach, judging by the high proportions of Ca and Mg that it leaches in the older rocks, attacks mainly carbonates, particularly calcite. The low carbonate contents (as calcite) in the younger rocks (Figure 7) is largely removed by the ammonium acetate leach (Figure 6.i) leaving little in the residue to be leached by the subsequent hydroxylamine leach.

Hydrochloric acid leach – elements contained in carbonates and monosulphides

Surprisingly, this leach was not so selective for carbonates, particularly calcite, and metal monsulphides like sphalerite, galena and pyrrhotite, as expected. In calcareous rocks, more than half the Ca (as calcite?) was dissolved by prior leaches (Figure 6). The HCl leach extracts little Mg in dolomite-rich rocks, but up to 30% of the Mg of other carbonate-rich rocks, perhaps suggesting that it is magnesian calcite and not dolomite that is attacked in these cases. This leach does not extract K (Figure 6). The proportions of Zn, Pb, Cu and Fe that this leach extracts tend to decrease with increasing age of the rocks (Figure 5A). A possible explanation for this trend is that with increasing burial depth the trace metals are incorporated into minerals of higher metamorphic grade that are more stable and more resistant to chemical attack compared to minerals from shallower burial depths.

Aqua regia leach minus sum of sequential leaches – elements contained in acid-soluble minerals

For the great majority of samples, it is this category that contains the bulk of Zn, Pb, Cu, Ni and Fe contained in the rock. Most of the Fe extracted is probably contained in ferro-magnesian minerals, particularly smectite and chlorite (see next section). Judging from the co-extraction association of Ca with Mg, this leach also dissolves dolomite and ankerite. Noting the low metal contents in carbonate-rich rocks (Figure 5), it is therefore likely that most of the metal mobilized occurred in chlorite and/or smectite in the original rock. Very little K is

extracted by this leach (Figure 6.i), attesting to the acid resistant properties of illite/muscovite* which likely contain the bulk of the K in these rocks. The small proportions that are mobilized are likely due to the attack of smectite in the younger rocks and biotite in the older, more metamorphosed rocks. In Devonian and younger rocks, 30-80% of the Na is leached by an aqua regia digestion, but very little is leached in the case in older rocks. The reason for this is that in the younger rocks, Na occurs in smectite, paragonite, plagioclase and, in the case of the Middle Valley samples, as sodium chloride of the original pore fluids, which are dissolved. In the older rocks, Na occurs almost exclusively in albite, which is resistant to an aqua regia digestion.

Residue from Aqua regia leach – elements contained in acid resistant minerals

This value was calculated as the difference between the whole rock "near total" content and the amount extracted by the aqua regia leach. It could have also be determined by the direct "near total" analysis of the aqua regia leach residue corrected for the weight loss of the solid reactant (rock powder) during aqua regia leaching. Both methods have their uncertainties because both use the results from two different methods of analysis. The results of both methods are very similar. The main minerals in the aqua regia residue are quartz, muscovite, albite, kaolinite, and minor minerals such as ilmenite, magnetite, rutile, etc. These acid resistant minerals general contain <10% of the Zn, Pb, Cu and Ni but on average contains 25% of the Fe and 90% of the Ba contained in the rock (Table 3).

Leach	Site of metals	Zn	Pb	Cu	Ba	Fe	Mn
1M Ammonium acetate	Clays	7.0	2.7	2.1	37.3	312.8	61.4
0.1M Sodium pyrophosphate	Organics	3.3	1.2	2.9	12.0	1,170.5	20.9
0.25M Hydroxylamine	Oxides	9.4	3.7	1.0	18.8	1,996.9	98.5
1M HCl	Carbonates and monosulphides	9.9	3.4	2.3	35.6	2,282.4	60.4
Aqua regia minus the sum of above sequential leaches	In minerals soluble in aqua regia	118.0	13.4	27.5	19.9	20,679.8	222.6
WR minus amount leached by aqua regia	In acid-resistant minerals	10.4	3.4	2.1	569.6	8,457.7	39.7
Average 60-100 mesh whole rock		147.0	23.0	35.0	652.0	32,618.0	440.0

Table 3. Average amounts of metals (in ppm) extracted by the different leaches and the sites in the rock where the metals are purported to occur.

* Because of the difficulty in distinguishing muscovite and illite by whole rock XRD in a rock that contains both (e.g. Verdel et al., 2011), muscovite and illite are referred to here as illite/muscovite in the text and as illite in diagrams.

Discussion

It is not surprising that there is much variation in the relative proportions of the siting and leachability of different metals and major elements of the samples used in this study, considering their different ages, provenances, depositional environments, and depths of burial which has controlled their present chemical and mineralogical compositions. Each sample is different, and responds differently to the different leaches. The generalizations made above are very broad and do not present general rules. In order to understand exactly what is happening during the different leaches, the data for each sample has to be analysed separately. At the time of writing, data analysis of individual samples is still being carried out. However, in order to give the reader insight into the methodologies of analysis, two examples are presented here and illustrated in Figures 8 and 9.

Sample LEA-12-ALB-2

Sample LEA-12-ALB-2 (Figure 8) is a dolomitic marl with oil-filled vugs from the Devonian Ireton Formation of western Alberta. The K-Mg-Ca ternary diagram shows the relative proportion of these elements in both the leachates and residues of the various experiments as indicated by the colour coding of the symbols. Other major elements listed in Figure 8D could also be used, but the plot shown gives the most spread of data across the diagram. As pointed out earlier, Si was not measured because of the low solubility of quartz in the leaches, and the use of sodium pyrophosphate as a leaching agent precludes the use of Na for analysing the leaching process. The solubility of Al in most leaches is usually limited by saturation with respect to kaolinite or dickite which collects in the insoluble residue, and therefore the amount of Al in the leachate is not a good measure of the amount of solubilisation of rock-forming minerals. Also shown on the diagram are the ranges of the relative proportions of K, Mg and Ca in the most common rock-forming minerals.

The SEM backscatter image (Figure 8B) and XRD analysis shows the sample to consist mainly of loosely packed dolomite grains with fine-grained quartz, illite/muscovite, and kaolinite in the interstices. The sample is oil-rich, and it is presumed that this also occupies the interstices. This dominance of dolomite in the sample is reflected in the high whole rock Ca and Mg contents (top row of Figure 8D) and the plotting of these whole rock contents close to the dolomite field in Figure 8A on a tie-line between dolomite and illite/muscovite. All leaches extract Ca and Mg in the same ratio that exists in dolomite which suggests that the main reaction occurring is the dissolution of dolomite, and not the selective leaching of adsorbed cations from different sites in the rock. If the leaching were from different adsorption sites then the ratios would not be constrained to those of mineral compositions. That the dissolution of dolomite is the main reaction for all leaches is substantiated by the compositions of the leach residues, which lie on a line from dolomite composition through the whole rock indicating the removal of dolomite. The residue of the aqua regia leach contains no dolomite (Figure 8A), consisting mainly of quartz, illite and kaolinite. The aqua regia
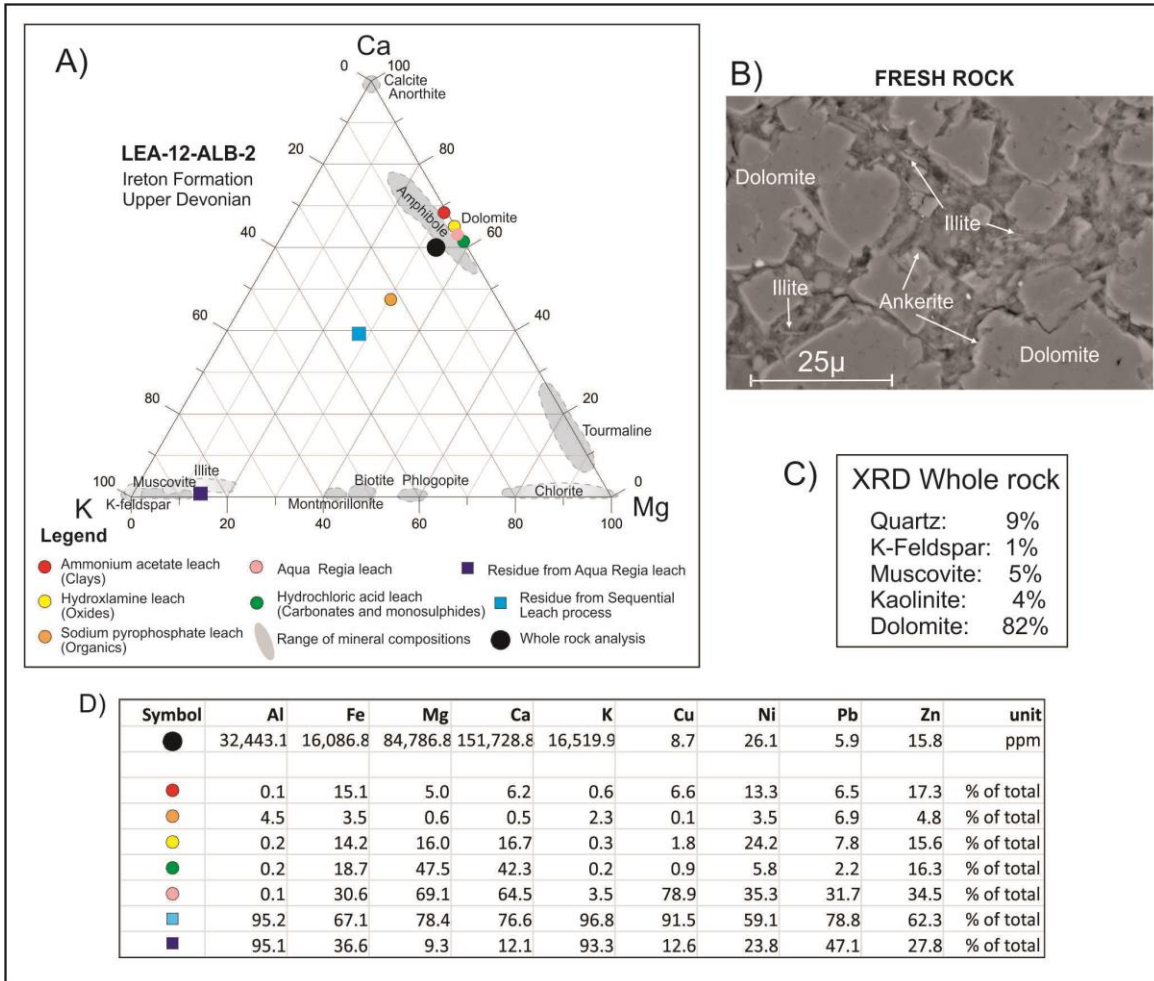
Figure 8. Summary of chemical and mineralogical analyses for sample LEA-12-ALB-2: A dolomite marl containing oil in vugs from the Upper Devonian Ireton Formation of western Alberta. A) Ternary K-Mg-Ca diagram showing relative proportion in leachates and residues of the 60-100 mesh fraction of a whole rock powder. Grey areas show the range of compositions of the indicated minerals from sedimentary basins (data from Lydon et al., 2000). B) SEM backscatter image of part of a rock grain prior to leaching. The rock is a porous dolomite with interstitial fine-grained dolomite, illite, and organics. C) Quantitative XRD analysis of whole rock powder. D) Summary of chemical compositions of the data points plotted in A). Top row is chemical composition of whole rock in ppm. Underlying five rows are the proportions of the indicated element extracted by the leach indicated by the symbol used in A), and the bottom row is the proportion of the elements that were not dissolved by aqua regia, calculated by subtracting the amount leached by aqua regia from the whole rock "near total" analysis. See text for discussion.
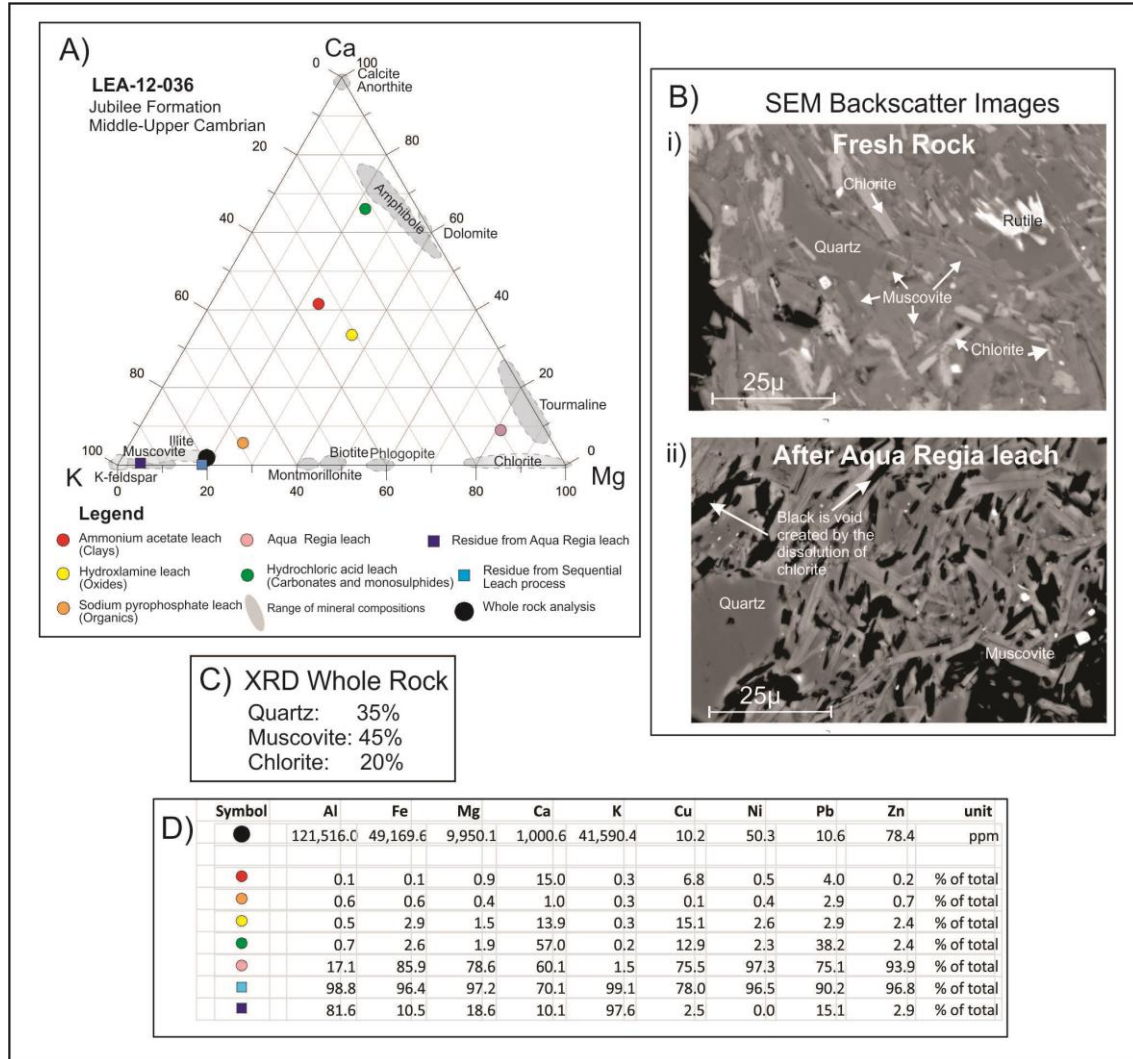
Figure 9. Summary of chemical and mineralogical analyses for Sample LEA-12-036-2: A shale layer from a nodular carbonaceous limestone from the Cambrian Jubilee Formation of British Columbia. A) Ternary Ca-Mg-K diagram showing relative proportion in leachates and residues of the 60-100 mesh fraction of a whole rock powder. Grey areas show the range of compositions of the indicated minerals from sedimentary basins (data from Lydon et al., 2000). B) SEM backscatter images of part of a rock grain: i) Prior to leaching. The rock is a muscovite-chlorite-quartz argillite. ii) After leaching with aqua regia. Note that chlorite has been dissolved even within the grain interior but the muscovite has not been corroded. C) Quantitative XRD analysis of whole rock powder, confirming the muscovite-chlorite-quartz composition of the rock. D) Summary of chemical compositions of the data points plotted in A). Top row is chemical composition of whole rock in ppm. Underlying five rows are the proportions of the indicated element extracted by the leach indicated by the symbol used in A), and the bottom row is the proportion of the elements that were not dissolved by aqua regia, calculated by subtracting the amount leached by aqua regia from the whole rock "near total" analysis. See text for discussion.

residue contains 93% of the K present in the original rock and illustrates that muscovite/illite is very resistant to chemical attack and thus unlikely to be a source of metals for SEDEX/MVT ore systems. The major repository of Fe in the sample is in the iron-rich rim of dolomite grains, (Figure 8B), which is presumably a diagenetic ankerite alteration. The ammonium acetate leach, the first of the sequential leaches, extracts three times the proportion of Fe as it does Mg or Ca, and this ratio decreases with each subsequent leach, suggesting that the sequential leaches progressively corrode the dolomite grains, removing the ankerite rim and exposing the dolomite to chemical attack. The ratio of the proportion of Zn to the proportion of Fe extracted is approximately 1:1 for all leaches, suggesting that most Zn in the rock occurs as a substitution for Fe in ankerite. This systematic covariation of Zn with Fe, Ca and Mg, is strong evidence supporting the interpretation that most of the cations that are leached from the rock is a result of mineral dissolution, and not elution of loosely bound ions on the surface of mineral grains.

Space does not permit a full discussion of the other metals here, but it is interesting to note that the sodium pyrophosphate leach, which purportedly attacks organic matter, failed to leach significant amounts of Ni, despite the presence of oil in the sample and the propensity for Ni to concentrate in oil (e.g. Hitchon, 1966; Hitchon and Filby, 1983; Magaw et al., 2000). However, the sodium pyrophosphate extracted 2.5% of the K in the rock, but little Mg and Ca. What mineral the sodium pyrophosphate attacked is unknown, but is possibly the K-Feldspar identified by whole rock XRD.

Sample LEA-12-036

In contrast to the carbonate-rich rock described above, sample LEA-12-036 is a shale from the Cambrian Jubilee Formation of eastern British Columbia, consisting mainly of quartz, muscovite and chlorite (Figure 9C), with, judging from its chemical response to leaching; Figure 9A) small amounts of a calcic phase which is probably calcite. The sequential leaches collectively extract only very small proportions (<6%) of rock components, except for Ca, Pb and Cu. Nearly all the Ca can be attributed to calcite dissolution, most of which was extracted by the HCl leach. About 40% of the Pb but very little Zn is extracted with the Ca by the HCl leach. As in sample LEA-12-ALB-2, the sodium pyrophosphate leach preferentially extracted K compared to other components. The great bulk of the ore metals is extracted by the aqua regia leach, which element ratios of Figure 9A and 9D indicate, mainly involves the dissolution of chlorite and small amounts of muscovite and a calcic phase. The almost complete dissolution of chlorite but acid resistance of muscovite is shown by the SEM backscatter images in Figure 9B which compares a grain of the fresh rock with a grain from the aqua regia leach residue. The conclusion is that most of the zinc in this rock is contained in chlorite, and is only released if the chlorite is altered or dissolved. This figure also demonstrates the very rapid inter-granular mass transfer that is possible due to instability between a rock forming mineral and a fluid, noting that the dissolution of chlorite is complete even in the centre of

the grain and is not confined to an alteration selvedge at the grain boundary. The response of this sample to the various leaches also illustrates the high resistance of a greenschist facies argillaceous rock to leaching, with 95% of the Zn and Ni, and 75% of the Cu and Pb, remaining in the rock after the sequential leaching process.
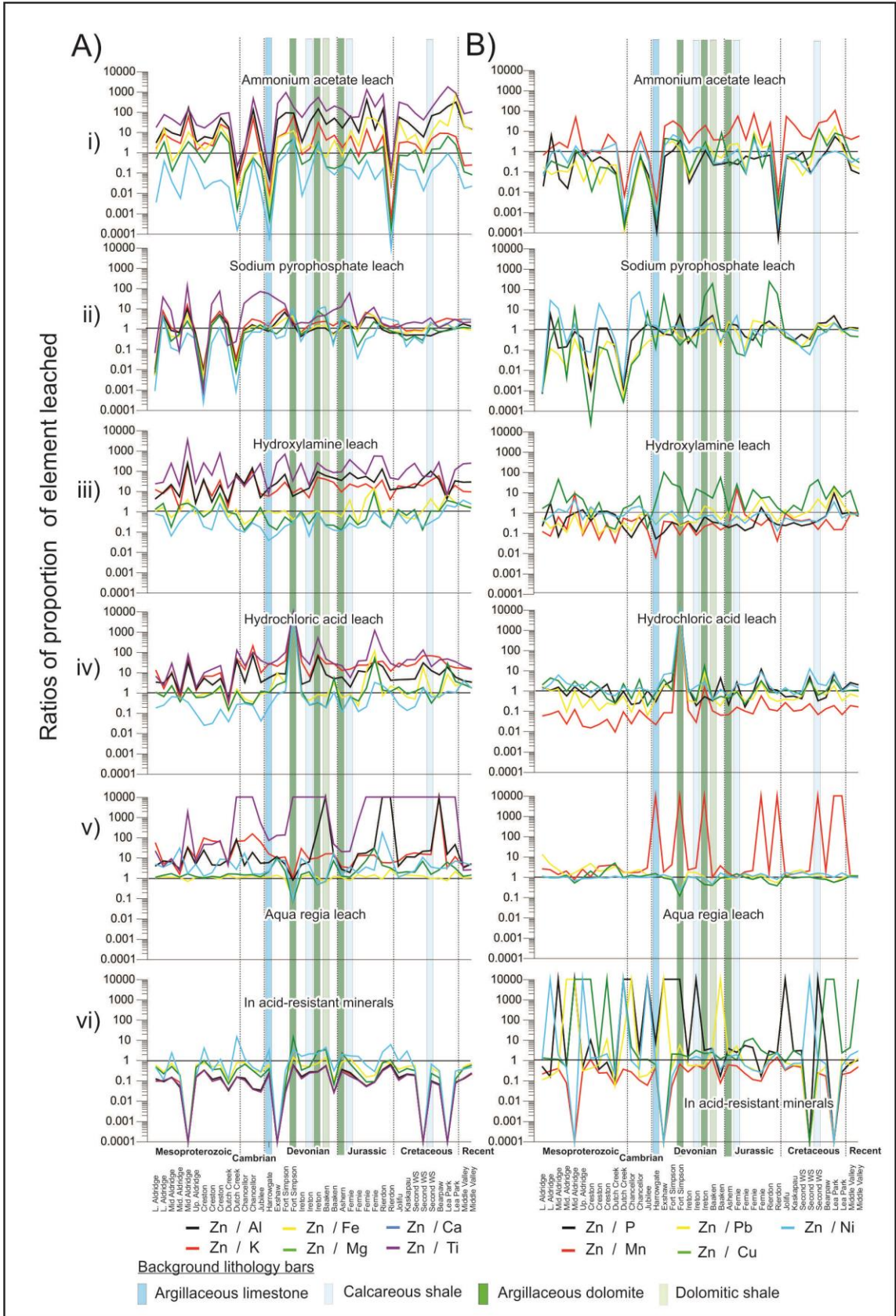
Proportion of Zn leached compared to proportions of other elements leached

The above examples both suggest that significant leaching of the metal content of a sedimentary rock involves the dissolution/alteration of rock forming minerals and therefore the metal reservoirs of the rocks are mainly within the structures of those rock-forming minerals. If this is universally the case then there should be a consistency in the ratios between a metal and the major elements of the rock forming minerals. Some variation can be expected because the same element can occur in more than one mineral.

The ratios of the proportion of Zn leached to the proportion of other elements leached are plotted in Figure 10. The column on the left has a major element as a denominator and the column on the right has a minor or trace element as a denominator. Points that plot above the line at the value of 1, signify that Zn is more leachable than the denominator element. Points that plot below the line at the value of 1, signify that Zn is less leachable than the denominator element. Samples that plot at the 10^4 value signify that the leachability of the denominator element is insignificant, whereas those that plot at the 10^{-4} value signifies that the leachability of Zn is insignificant, and usually due to very low Zn contents in the sample.

In general, there are certain consistencies to the ratio for the proportion of Zn extracted compared to the proportion of major element extracted (Figure 10A). For the great majority of samples and leaching method, the proportion of major element leached is in the order Ca>Mg>Fe>K>Al>Ti. This consistent order of the major elements suggests that their extractability of the major element is controlled by the relative solubilities of the mineral(s) containing the major element and not the more random quantity of the elutable amount of the element adsorbed on to substrate. This order of elements changes only for the aqua regia leach, where Ca is less leachable than Mg and Fe. The reason for this is likely because the HCl leach removes most of the calcite in the rock, leaving only the less soluble dolomite, plagioclase and perhaps amphibole for the aqua regia leaching.

The ratio of 1, which indicates that Zn and the major elements are leached in the same proportions by dissolution of a rock forming mineral containing the denominator element(s), is most consistent for Fe (Figure 10A.v) particularly for the aqua regia leach which extracts ~70% of Zn for most rocks. This indicates that most commonly Zn substitutes for Fe in minerals of sedimentary rocks. For aqua regia leaching of Paleozoic rocks, the Zn/Mg ratio is also close to 1,

(Figure caption is on next page.)

Figure 10. The proportion of Zn extracted compared to the proportion of major elements extracted by different leaches in Column A and compared to the proportion of other trace elements in Column B. A value of 1 indicates that zinc and the denominator element are extracted in the same proportion, likely indicating that both are exclusively hosted by the same mineral. Values of >1 indicate that Zn is more leachable than the denominator element, and values <1 indicate that the denominator element is more leachable than Zn. See text for discussion.

indicating that Zn, Fe and Mg are proportionally extracted from the same mineral. As seen above for sample LEA-12-036, this is due to the dissolution of chlorite. The Zn/Mg ratio rocks is higher than the Zn/Fe of Mesozoic rocks by aqua regia leaching, probably because proportionally more Mg than Fe is leached by the first four sequential leaches (compare Figure 6A.ii and iii) and a higher proportion remains in the aqua regia residue as illite (judging from ternary K-Fe-Mg plots). The general gradual trend of decreasing proportions of Fe and Mg leached by the first four sequential leaches (Figure 6A.ii and A.iii) is consistent with the diagenetic change from illite-smectite to muscovite with increasing depth of burial. This suggests that because of the stability of muscovite, the proportion of Zn that can be extracted by weak leaches from argillaceous rocks, decreases with increasing depth of burial. This suggestion is corroborated by Figure 5A.i and 5B.i. This pattern is the opposite for Pb, which shows a trend of increasing tendency for extraction by weaker leaches with increasing depth of burial (Figure 5A.ii and 5B.ii). This difference in leaching response with increasing depth of burial of source rocks, may be the basis for the range of Zn:Pb ratios of SEDEX and MVT deposits.

The extractability of Zn compared to other metals (Figure 5B) depends upon the leach, and for the weaker leaches, upon the sample. For the ammonium acetate and sodium pyrophosphate leaches, generally the leachability follows the order Cu>Pb>P>Zn>Ni>Mn for Mesoproterozoic rocks and Cu>Ni>P>Zn>Pb>Mn for Mesozoic rocks, but with so much variability the validity of this generalization could be questioned. The relative extractability of metals is much more consistent for the hydroxylamine and hydrochloric acid leaches, with only Mn being consistently the most extractable for most samples. The metal ratios for the aqua regia leach are close to 1 for most samples, meaning that if Zn is contained mainly in smectite-chlorite at shallow burial depths and chlorite at greater burial depths, so are all the other metals. The zero values for P and Mn are artifacts of the method of calculation for the amounts of metal that would be removed by the aqua regia leach if it were in reality the last of the sequential leaches (see above) and not, as was the case, a separate leach of rock powder.

Conclusions
The data presented here emphasizes that trace metals in rocks are contained mainly within the structure of rock-forming minerals. The consistency between the amounts of metals leached and the amounts of major elements leached questions whether rocks contain significant quantities of metals that are loosely

adsorbed on to a substrate. The data can also be used to question the assumption that the selective leaches used here are specific to the sites claimed for them when it comes to leaching rock powders. Although the sequential leach data for metals could be interpreted in accord with the conclusions of Zielenski et al. (1983) to indicate that metals supposedly adsorbed on to the surfaces of clays, organic matter, and/or iron and manganese oxides are readily leached to give concentrations sufficient to form ore deposits, the co-analysed major element data puts constraints on the applicability of the experimental leaching to natural systems. This major element data indicates that the major rock-forming elements are solubilized in about the same proportions as the metals, meaning that most of the metal content of sedimentary rocks is as diadochic substitutions or micro mineral inclusions in the rock forming minerals. In other words, to extract the 10-20% of metal content of the rock that weak selective leaches achieve (e.g. Zielenski et al., 1983), >10-20% of the rock would have to be dissolved or at least thoroughly altered by the same volume of fluid. As Lydon (1986) pointed out, this is impossible because the fluid would lose its reactive capacity even before <1% of the source rock was altered. This would imply that the availability of leachable metals in sedimentary basins is not a limiting control on the generation of SEDEX/MVT ore systems.

Bearing in mind the constraints of the major element data, the analyses presented here leads to conclusions similar to that of Bischoff et al. (1981):

1. The amount of metal that can be leached from a sedimentary rock is proportional to the amount of dissolution or alteration of the source rock and the concentration of metals in the rock-forming minerals.
2. The maximum amount of metal in the pore fluid depends on the concentration of metal-complexing ligands, particularly chloride, in the fluid, the temperature of the pore fluid, and the saturation limit with respect to a metallic mineral.

These conclusions point to further implications:
3. The need for chloride brines to leach metals to produce a SEDEX/MVT ore system, which, as the evidence noted above indicate are evaporated sea water, means that the sedimentary basin must have been at low latitudes adjacent to an extensive shallow continental shelf, at some time in its history.
4. Because the leaching of significant amounts of metal by pore fluids requires the alteration of the source rocks beyond the reactive capacity of a pore fluid to achieve, extraction of significant amounts of metals can only be accomplished during leaching windows afforded by metamorphic mineral-mineral reactions.
5. Considering that fluid inclusion filling temperatures for SEDEX/MVT deposits is generally <200°C (e.g. Wilkinson, 2001), the most likely metamorphic reaction zone is the 90-100°C of the smectite-illite transformation of the second dehydration event of Burst (1969).

Implications for Exploration

The implications of the results of this work for the generation of SEDEX/MVT ore systems are twofold:

1. Metal leaching in SEDEX/MVT systems is restricted to windows of mineral transformations during diagenesis. Because at normal water-rock ratios the reactive capacity of the pore fluids of a sediment are exhausted before any significant volume of rock is solubilized or altered, the only viable mechanism for leaching large quantities of metal is during the mineralogical transformations afforded by P-T driven metamorphic reactions (i.e. source rock alteration is driven by mineral-mineral disequilibrium and not by fluid-mineral disequilibrium).

2. SEDEX/MVT ore systems can develop only in those sedimentary basins with a prior history of evaporitic conditions. Because high concentrations of Zn and Pb in natural fluids are possible only in chloride brines, and large amounts of chloride brines can only be generated by solar evaporation of sea water, it follows that the sedimentary basin or adjacent platform must have experienced evaporitic conditions at some time during its history.

These two concepts severely restrain genetic models for SEDEX/MVT ore systems, and hence the exploration strategies based on these models. For example, basins that have not experienced low latitude climatic conditions at some time in its history, nor is adjacent to an extensive shallow water shelf on which evaporitic conditions can develop, are unlikely to be fertile for the development of a SEDEX/MVT ore system. The stratigraphic level at which evaporitic brines may have developed is the oldest stratigraphic level in the sedimentary basin at which SEDEX deposits can form. The restriction of metal leaching to windows of diagenetic mineral transformations, gives rise to the possibility of using the halide or base metal contents of minerals formed during these windows, such as apatite, ilmenite, etc., as a means for testing a basin for the former presence of metalliferous brines. In other words, this work brings a new perspective of how and when metalliferous brines are formed, and opens up new directions for both exploration strategies and exploration techniques.

Future Work

The large amount of data generated by this study has the capacity to yield further insights into the mobility of metals in sedimentary basins upon continued and further analysis. Important to future work in understanding SEDEX/MVT system, as alluded to several times above, is the relationship between the formation of metalliferous brines and the maturation of kerogens to form oil and gas, and the co-migrations of these fluids in the sedimentary basin. Collaboration between metallogenists with oil geologists would undoubtedly give more realistic insights into the hydrodynamic architecture and evolution of sedimentary basins. With this connection in mind, possible new insights might include using vanadium as a geochemical vector to SEDEX vent field, noting that any structure that allows the upward escape of metalliferous brines must also allow the upward escape of oil and gas and form a dispersion plume of metals contained in the oil. Since brine

fields are density stratified and the halogen ratios of evaporated seawater are related to density (e.g. Worden, 1996), mapping of the halogen contents of, say, apatite might be a way to determine whether a basin contained brine during the leaching windows of diagentic mineral transformations.

This work also brings to attention other questions on SEDEX/MVT systems which need research. If metal leaching requires high density brines, then what is the mechanism to bring these brines to the sea floor? It cannot be convection, because fluid inclusions of SEDEX deposits suggest maximum temperatures of ~200ºC (e.g. Wilkinson, 2001), which is too low for >18 wt.% NaCl brines to become buoyant in sea water.

Acknowledgements

References

Bischoff, J.L., Arthur S. Radtke, A.S., and Robert J. Rosenbauer, R.J., 1981, Hydrothermal alteration of graywacke by brine and seawater: roles of alteration and chloride complexing on metal solubilization at 200º and 350ºC: Economic Geology, v. 76, p. 659-676.

Burst, J.F., 1969, Diagnosis of Gulf Coast clayey sediments and its possible relation to petroleum migration: Bulletin of the American Association of Petroleum Geologists, v. 53, p. 73-93.

Carpenter, A.B., Trout, M.L., and Pickett, E.E., 1974, Preliminary report on the origin and chemical evolution of lead- and zinc-rich oil field brines in Central Mississippi: Economic Geology, v. 69, p. 191-206.

Cathles, L.M., and Smith, A.T., 1983, Thermal constraints on the formation of Mississippi Valley–Type lead-zinc deposits and their implications for episodic basin dewatering and deposit genesis: Economic Geology, v. 78, p. 983-1002.

Chao, T.T., 1984, Use of partial dissolution techniques in geochemical exploration: Journal of Geochemical Exploration, v. 20, no. 2, p. 101-135.

Ellis, A. J., 1968, Natural hydrothermal systems and experimental hot water/rock

interaction: Reactions with NaCl solutions and trace metal extraction: Geochimica et Cosmochimica Acta, v. 32, p. 1356-1363.

Emsbo, P., 2009, Geologic criteria for the assessment of sedimentary exhalative (SEDEX) Zn-Pb-Ag deposits: United States Geological Survey, Open-File Report 2009-1209, 21 p.

Garrels, R.M., and F.T. Mackenzie, 1971, Evolution of sedimentary rocks: W.W. Norton & Co., New York. 397 p.

Garven, G., and Freeze, R.A., 1985a, Theoretical analysis of the role of groundwater flow in the genesis of stratabound ore deposits: 1. Mathematical and numerical model: American Journal of Science, v. 284, p. 1075-1124.

Garven, G., and Freeze, R.A., 1985b, Theoretical analysis of the role of groundwater flow in the genesis of stratabound ore deposits: 2. Quantitative results: American Journal of Science, v. 284, p. 1125-1174.

Goodfellow, W.D., and Lydon, J.W., 2007, Sedimentary exhalative (SEDEX) deposits, in Goodfellow, W.D., ed., Mineral deposits of Canada: A synthesis of major deposit-types, district metallogeny, the evolution of geological provinces, and exploration methods: Geological Association of Canada, Mineral Deposits Division, Special Publication no. 5, p. 163-184.

Hanor, J.S., 1996, Controls on the solubilization of lead and zinc in basinal brines, in Sangster, D.F., ed., Carbonate-hosted lead-zinc deposits: Society of Economic Geology, Special Publication no. 4, p. 483–500.

Hitchon, B., 1966, Formation fluids, Chap. 15 in Geological history of western Canada: Calgary, Alberta: Alberta Society of Petroleum Geologists, p. 201-217.

Hitchon, B., Billings, G.K., and Klovam, J.E., 1971, Geochemistry and origin of formation waters in the Western Canada basin-III. Factors controlling chemical composition: Geochimica et Cosmochimica Acta, v. 35, p. 567-598.

Hitchon, B., and Filby, R., 1983, Geochemical studies – trace elements in Alberta crude oils: Alberta Research Council for Alberta Energy and Utilities Board and Alberta Geological Survey, Open File report 1983-02, 150 p.

Kharaka, Y.K., Maest, A.S., Carothers, W.W., Law, L.M., Lamothe, P.J., and Fries, T.L., 1987, Chemistry of metal-rich brines from Central Mississippi salt dome basin, U.S.A.: Applied Geochemistry, v. 2, p. 543-561.

Leach, D.L., Sangster, D.F., Kelley, K.D., Large, R.R., Garven, G., Allen, C.R., Gutzmer, J., and Walters, S., 2005, Sediment-hosted lead-zinc deposits; a global perspective, in Hedenquist, J.W., Thompson, J.F.H., Goldfarb, R.J., and Richards, J.P., ed., Economic Geology, 100th anniversary volume, 1905-2005: Littleton, CO, Society of Economic Geologists, p. 561-607.

Lentini, M. R., and Shanks, W. C., III, 1983, Experimental study of brine-arkose interaction at 200 degrees C and 500 bars; origin of metalliferous oil field brines and Mississippi valley-type ore deposits, in Kisvarsanyi, G., Grant, S.K., Pratt, W. P., and Koenig, J. W., ed., International Conference on Mississippi Valley-type lead-zinc deposits: Proceedings volume, Rolla, MO, University of Missouri-Rolla, p. 195-205.

Long, D.T., and Angino, D.T., 1982, The mobilization of selected trace metals from shales by aqueous solutions: effects of temperature and ionic strength: Economic Geology, v. 77, p. 646-652.

Lydon, J.W., 1983, Chemical parameters controlling the origin and deposition of

sediment-hosted stratiform lead-zinc deposits: Mineralogical Association of Canada Short Course Handbook, v. 8, p. 175-250.

Lydon, J.W., 1986, Models for the generation of metalliferous hydrothermal systems within sedimentary rocks and their applicability to the Irish Carboniferous Zn-Pb deposits, *in* Andrew, C.J., Crowe, R.W.A., Finlay, S., Pennell W.M., and Pyne, J.F., ed., The geology and genesis of mineral deposits in Ireland: Irish Association of Economic Geology and Geological Survey of Ireland, p. 555-577.

Lydon, J.W., Walker, R., and Anderson, E.H., 2000, Lithogeochemistry of the Aldridge Formation and the chemical effects of burial diagenesis, *in* Lydon, J.W., Höy, T. ,Slack, J.F., and Knapp, M.E., ed., The geological environment of the Sullivan deposit, British Columbia: Geological Association of Canada, Mineral Deposits Division, Special Publication no. 1, p. 136-179.

Magaw, R.I., McMillen, S.J., Gala, W.R., Trefry, J.H., and Trocine, R.P., 2000, Risk evaluation of metals in crude oils, *in* Sublette, K.L., ed., Proceedings of the 6th International Petroleum Environmental Conference, Houston, TX: SCG Inc., p. 460-473.

Milliken, K.L, 2004, Late diagenesis and mass transfer in sandstone and shale Sequences, *in* Holland, H.D., and Turekian, K.K., ed., Treatise on Geochemistry: Elsevier, Amsterdam, v. 7, p. 159-190.

Rittenhouse, G., Fulton, R.B., Grabowski, R.J., and Bernard, J.L., 1969, Minor elements in oil-field waters: Chemical Geology, v. 4, p. 189-209.

Roedder, E., 1984, Fluid inclusions: Mineralogical Society of America, Reviews in Mineralogy, v. 12, 644 p.

Russell, M.J., 1978, Downward-excavating hydrothermal cells in Irish type ore deposits: importance of an underlying thick Caledonian prism: Transactions Institute Mining and Metallurgy, v. 87, p. B168–171.

Russell, M.J., Solomon, M., and Walshe, J.L., 1981, The genesis of sediment-hosted, exhalative zinc + lead deposits: Mineralium Deposita, v. 16, p. 113-127.

Samson, I.M., Russell, M.J., 1987, Genesis of the Silvermines zinc–lead–barite deposit, Ireland: fluid inclusion and stable isotope evidence: Economic Geology, v. 82, p. 371–394.

Sverjensky, D.A., 1984, Oil field brines as ore-forming solutions: Economic Geology, v. 79, p. 23–37.

Turekian, K.K., and Wedepohl, K.H., 1961, Distribution of the Elements in some major units of the Earth's crust: Geological Society of America Bulletin, v. 72, p. 175-192.

Viets, J.G., Hofstra, A.H., and Emsbo, P., 1996, Solute compositions of fluid inclusions in sphalerite from North American and European Mississippi Valley-type ore deposits: ore fluids derived from evaporated seawater, *in* Sangster, D.F., ed., Carbonate-hosted lead–zinc deposits: Society of Economic Geology Special Publication no. 4, p. 465-482.

Verdel, C., Niemi, N., and van der Pluijm, B.A., 2011, Variations in the illite to muscovite transition related to metamorphic conditions and detrital muscovite content: insight from the Paleozoic passive margin of the southwestern United State: Journal of Geology, v. 119, p. 419–437.

Weiss, A., and Amstutz, G.C., 1966, Ion-exchange reactions on clay minerals and cation selective membrane properties as possible mechanisms of economic metal concentration: Mineralium Deposita, v. 1, p. 60-66.

Wilkinson, J.J., 2001, Fluid inclusions in hydrothermal ore deposits: Lithos, v. 55, p. 229–272.

Worden, R.H., 1996, Controls on halogen concentrations in sedimentary formation waters: Mineralogical Magazine, v. 60, p. 259-274.

Yang, J., Large, R.R., Bull, S., and Scott, D.L., 2006, Basin-scale numerical modeling to test the role of buoyancy-driven fluid flow and heat transfer in the formation of stratiform Zn-Pb-Ag deposits in the northern Mount Isa Basin: Economic Geology, v. 101, no. 6, p. 1275-1292.

Zielinski, R.A., Bloch, S., and Walker, T.R., 1983, The mobility and distribution of heavy metals during the formation of first cycle red bed: Economic Geology, v. 78, no. 8, p. 1574-1589.